ISSN1027-5495. Functional Materials, 30, No.4 (2023), p. 511-518
doi:http://dx.doi.org/10.15407/fm30.04.511

Structural and morphological changes in $FeCl_3$-modified carbon material

V.M. Vashchynskyi, I.V. Semkiv, M.V. Solovyov, H.A. Ilchuk

Lviv Polytechnic National University, 12 S. Bandery Str., Lviv, 79013, Ukraine

Received August 30,2023

The work describes the three-step modification process including 1) impregnation of the carbon-containing precursor with $FeCl_3$; 2) heat treatment in an argon atmosphere at 700 C; 3) washing with distilled water and drying of samples to remove the residual activating agents and by-products of the reaction. The characteristics of carbon such as porosity, the chemical composition of the surface, and sorption properties have been thoroughly analyzed. The features of the formation of inclusions on the surface of the original carbon material CSTR-08 have been investigated using scanning electron microscopy, and their nature has been established. The main parameters of the specific surface, namely the total surface area, the total volume, and the average pore radius were determined by the methods of adsorption porosimetry and small-angle X-ray scattering. It has been found that the $FeCl_3$ modification of the carbon material leads to a three-fold increase in the material density and an increase in the number of pores with a radius of 25-50 Å. The high specific surface area (S =1875 m^2/g) allows the $FeCl_3$-modified material to be used as a favorable adsorbent in the aqueous phase, and the presence of stable and well-dispersed iron species on the carbon surface makes it a promising catalyst.

Keywords: porous carbon material; chemical activation; iron chloride; pore radius.

Структурно-морфологічні зміни вуглецевого матеріалу, модифікованого $FeCl_3$.
В.М. Ващинський, І.В. Семків, М.В. Соловйов, Г.А. Ільчук

Описується спосіб модифікації, який складається з трьох різних етапів: 1) просочування вугецевовмісної сировини $FeCl_3$; 2) термічна обробка в атмосфері аргону при 700 °C; 3) промивання дистильованою водою та сушіння зразків для видалення решти активуючих агентів і побічних продуктів реакції. Детально проаналізовано характеристики вуглецю щодо пористості, хімічного складу поверхні та сорбційних властивостей. За допомогою растрової електронної мікроскопії досліджено особливості утворення включень на поверхні вихідного вуглецевого матеріалу CSTR-08 та встановлено їхню природу. Методами адсторбційної порометрії та малокутового рентгенівського розсіяння визначені основні параметри питомої поверхні, а саме загальна площа поверхні, сумарний об'єм та середній радіус пор. Встановлено, що модифікація $FeCl_3$ вуглецевого матеріалу призводить до збільшення густини матеріалу втричі та збільшення кількості пор радіусом 25-50 Å. Велика питома площа поверхні (S=1875 $м^2/г$) дозволяє використовувати матеріал, модифікований $FeCl_3$ як перспективний адсорбент у водній фазі, а наявність стабільних і добре розподілених форм заліза на поверхні вуглецю робить його перспективним каталізатором.

1. Introduction

Porous carbon materials (PCMs), characterized by a large specific surface area [1], high porosity [2], physicochemical stability [3], and excellent surface reactivity [4], are widely used as functional materials for various applications, related to human and environmental safety, as well as in the energy industry [5], process and chemical manufacturing [6]. They are of great practical importance when applied in adsorption processes [7] and when serving as an electrode component for electrical energy storage systems [8]. In this regard, most PCMs

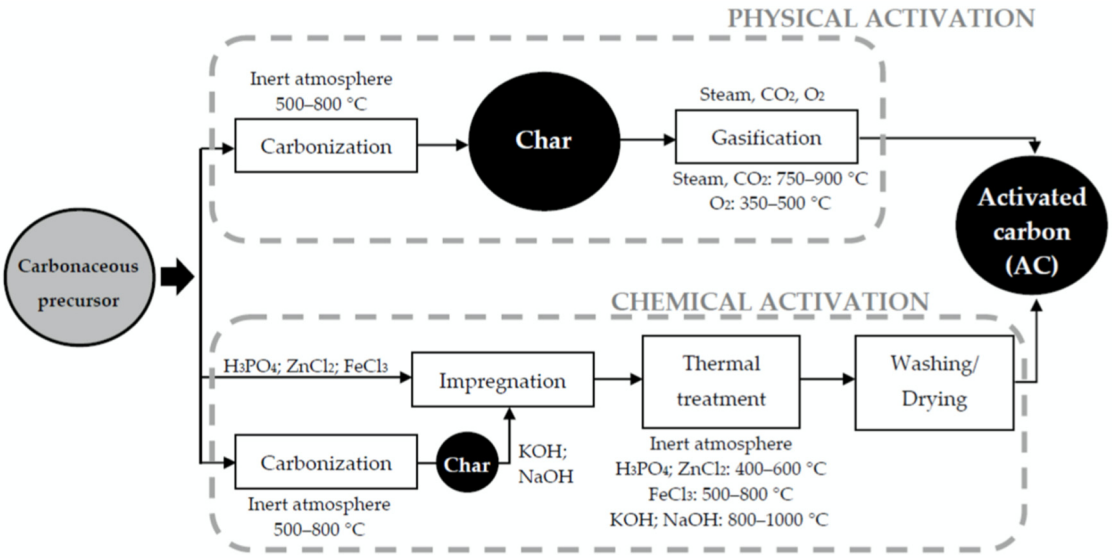

Fig. 1. Stages of PCM synthesis

have heterogeneous, predominantly microporous structures, which is sufficient for their use as sorbents in various industrial, medical, or analytical chemistry fields. At the same time, electrodes are manufactured with the help of PCM in electrochemical capacitors for electrical energy storage systems and fuel cells. It is characteristic that a developed mesoporous carbon surface, wide pore size distribution, and a sufficient number of transport pores are important to be used for this industry [9]. Therefore, the study of the process of PCM synthesis is of crucial scientific and practical significance.

There are two different methods of PCM obtaining, specifically physical activation and chemical activation (Fig. 1) [10, 11]. The first one is the pyrolysis or carbonization of a carbonaceous precursor at high temperatures, typically in the range of 700-900° C, in an inert atmosphere to avoid combustion of the carbonaceous material. At this stage, heteroatoms are removed and volatile substances are released, resulting in carbon matter with a high carbon content (the increase of the carbonization temperature increases the carbon content) but with a low-developed porous surface. This drawback then can be eliminated at the gasification stage. The most reactive carbon atoms, which generate the characteristic porosity of the material, are selectively removed with the help of controlled gasification reactions.

Another procedure for synthesizing PCM is chemical activation. This method is multistage, involving one thermal stage and two chemical treatment stages of carbon-containing feedstock. During the first stage, the precursor is impregnated with an activator. Various activating agents are traditionally explored in the literature, such as $ZnCl_2$, H_3PO_4, NaOH, or KOH. Among them, $FeCl_3$ has gained significant interest in recent years. The use of $FeCl_3$ offers certain advantages compared to other more conventional chemical reagents. For instance, it is cost-effective and more environmentally friendly. Other traditional activators like KOH, NaOH, or H_3PO_4 are strong bases and acids. The application of these materials requires strict safety measures and more corrosion-resistant materials, thus increasing the cost of the synthesis process. In the case of $ZnCl_2$, Zn ions and derived oxides are toxic [12, 13], necessitating stringent operational guidelines. All these factors indicate that $FeCl_3$ activation can be considered cost-effective and environmentally safer compared to traditional activating agents.

The procedure of impregnating carbon materials with $FeCl_3$ can be carried out using various methods. For instance, some researchers [14] employ an aqueous solution of the activating agent that comes into contact with the carbonaceous precursor. However, other studies perform a direct and simpler physical mixing of the activating agent and the precursor. One of the most crucial parameters with regard to its impact on the final PCM texture is the impregnation ratio or the mass ratio between the activating agent and the carbonaceous precursor. Impregnation ratios ranging from 0.5 to 5 are commonly encountered in the literature. After impregnation, the second step of the chemical activation process involves heat treatment in an inert atmosphere at different temperatures depending on the chosen activator. As shown in Fig. 1, the choice of temperature depends on the activating agent. During this stage, depolymerization, dehydration, and condensation reactions occur, leading to a higher carbon yield compared to physical activation due

to the limited formation of resins and volatile compounds. Eventually, the last stage involves washing and drying the samples to remove any remaining activating agents and by-products of the reaction that may block the newly formed porous surface. During NaOH or KOH activation of carbon precursors, such as biomass waste, an initial carbonization stage is usually required; as otherwise, these strong alkalis may dissolve the organic material of the precursor, preventing further activation [15].

Considering the variety of methods of thermal and chemical modification and other important nuances in obtaining carbon materials, there is a need for a detailed investigation of the aforementioned stages. Thus, the main objective of this work is to study the structural and morphological properties of porous carbon material and to assess the influence of iron chloride as a chemical activator on the porous structure and size distribution of carbon pores.

2. Experimental

The initial carbon material used for the examination has been manufactured at the National Institute of Coal (Oviedo, Spain) and designated CSTR-08. The modification of the investigated carbon matter has been conducted in several stages. In the first stage, optimal conditions for chemical activation have been selected based on the literature data [16]. The studied carbon material has been mechanically ground to a fraction of 200-250 μm, soaked in an aqueous solution of ferric chloride in a weight ratio of X_C = 2:3, where $X_C = m(\mathrm{C})/m(\mathrm{FeCl_3})$, and left for 24 hours. Subsequently, it has been dried in a thermostat to a constant weight at 100°C. The next stage has involved thermal activation of the modified matter in an inert atmosphere at 700°C for 90 minutes by introducing a water aerosol with argon into the reactor.

The resulting carbon was subjected to three rounds of washing by boiling in distilled water. The solid products of thermolysis were washed in distilled water for 30 minutes until a neutral pH to remove mineral impurities and ash. Subsequently, they were dried in a drying oven to a constant weight.

The surface morphology and elemental composition of the samples were investigated using a scanning electron microscope (SEM) model REMMA-102-02 (Selmi, Ukraine) equipped with an energy-dispersive microanalyzer. Small-angle X-ray scattering spectra were measured using a DRON-3 X-ray diffractometer with CuKα radiation (λ =1.5418 Å) monochromatized by reflection from the (200) plane of a LiF single crystal. The measurements were performed in the transmission mode, with X-ray radiation passing through the sample. The output signals of the detector were analyzed using the UEVU-3M electronic computing complex connected to a computer. Collimators for the primary and scattered beams were used to reduce parasitic scattering from the single crystal monochromator and entrance slits, as well as to decrease the intensity of background scattering. The collimation system makes it possible to measure small-angle scattering spectra starting from s = 0.1 nm^{-1}, where .. is the wave vector and 2Θ is the scattering angle. The width of the receiving slit of the detector was 0.1 mm providing an angular resolution of $\Delta 2\Theta$ = 0.03. Scattered radiation was registered in a scanning mode with a step of 0.05° and an exposure time of τ = 125 s. In the area of the smallest scattering angles, the scattered radiation overlays the primary beam, attenuated by absorption in the sample. To determine the actual material density, the following formulas were used:

$$\rho_m = \frac{\ln\left(\frac{I_0}{I}\right)}{\mu d} \quad (1)$$

$$w = 1 - \frac{\rho_m}{\rho_x} \quad (2)$$

Here I – is the intensity of the primary beam without a sample; I is the intensity of the primary beam with a sample; $\rho_x \approx 1.9$ g/cm^3 is the structural density of the sample.

The structural and adsorption characteristics of porous materials were studied by nitrogen sorption at a temperature of T = 77 K on an automated Quantachrome Autosorb sorptometer (Nova 2200e). The samples have been predegassed under vacuum at 453 K for 20 hours. The pore size distribution has been determined using the Density Functional Theory (DFT) method.

3. Results and discussion

Microphotographs of carbon sample CSTR-08 at different magnifications of the surface, grains, and micro-pores located within the grains are shown in Fig. 2. At low magnifications (×100 and ×200), surface inhomogeneity is observed. A mixture of grains with irregular geometric shapes and varying sizes is visible, ranging from fractures smaller than 0.5 μm. Isolated, close to flat formations with a length of 100 microns are found. Grains with irregular shapes, characterized by sizes of 40–60 μm, have pores randomly distributed on their surfaces. Smaller grains with pore fragments of regular geometric shapes on the surface could

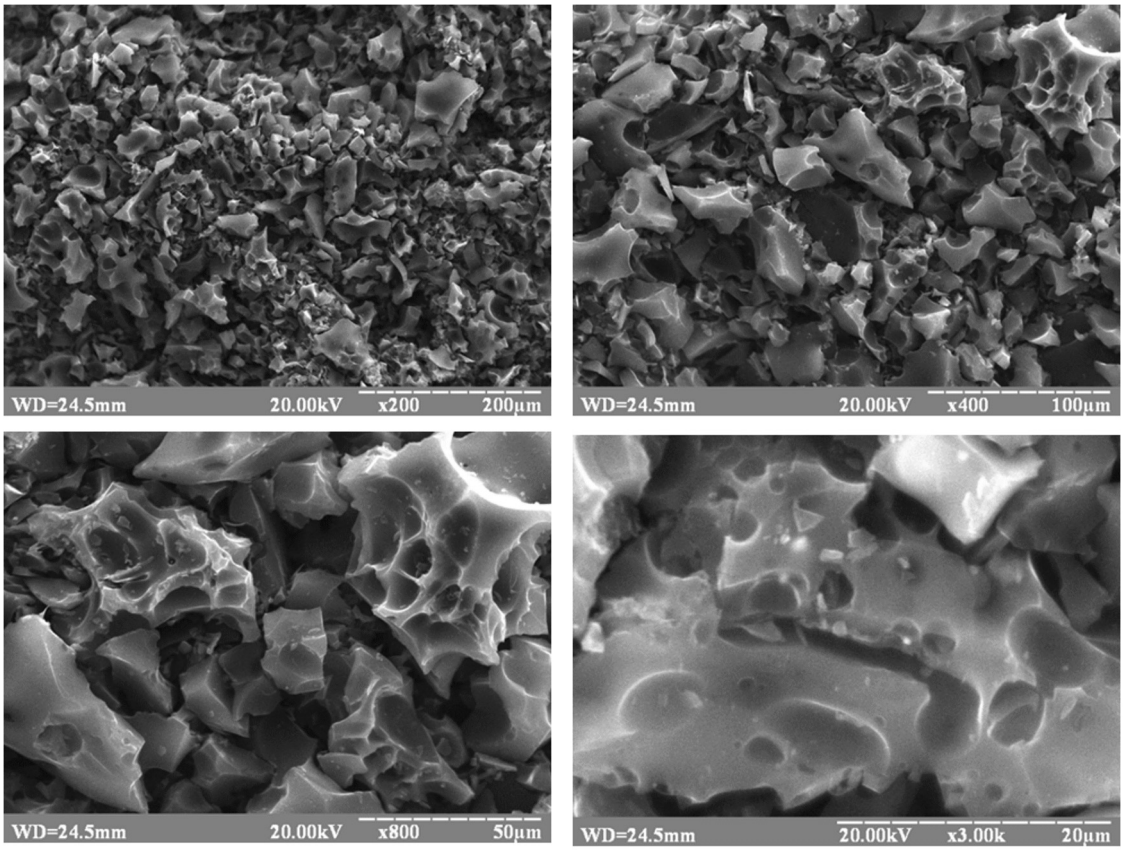

Fig. 2. Microphotographs of surface of porous carbon material CSTR-08 at different magnifications

have formed as a result of the mechanical breakdown of larger fragments.

The pores exhibit a regular geometric shape similar to etching pits in the isotropic material. Their uneven distribution becomes evident at higher magnifications. Two groups of pores with average diameters of 1.5±0.4 µm and 10±3 µm are observed in the CSTR-08 samples. Defects resulting from the merging of several pores have dimensions exceeding 30 µm and serve as grain shape components.

Before the chemical activation of carbon material CSTR-08, an integral analysis of the elemental composition has been conducted (Fig. 3). The applied accelerating voltage allowed analysis to a depth of up to 1 µm. The following chemical elements have been identified: O in bound form, Si, S, Cl, and Cr. The grains with inclusions of the Cr_2O_3 compound were also found within the pores (Fig. 2). The Cr content was 0.12±0.03 wt%. The total content of all impurities was 9 wt% (Table 1).

The influence of the chemical activator $FeCl_3$ on the porous structure and density of the carbon material were studied using the small-angle (X-ray or Neutron) scattering method (SAS). The intensity curves are presented in Fig. 4a (carbon material CSTR-08) and Fig. 4b (CSTR-08 modified with $FeCl_3$). A common feature of both samples is the presence

Table 1. Spectral dependence of characteristic X-ray emission (c) integrally collected from represented sample area (a)

Element	Peak intensity	Error, %	Content, wt %	Content, atom %
O	985	3.15	8.33	8.6965
Si	280	10.09	0.18	0.1049
S	150	17.31	0.1	0.0543
Cl	161	16.3	0.09	0.0408
Ca	284	8.74	0.21	0.0857
Cr	92	19.17	0.12	0.038
Sum			9.02	

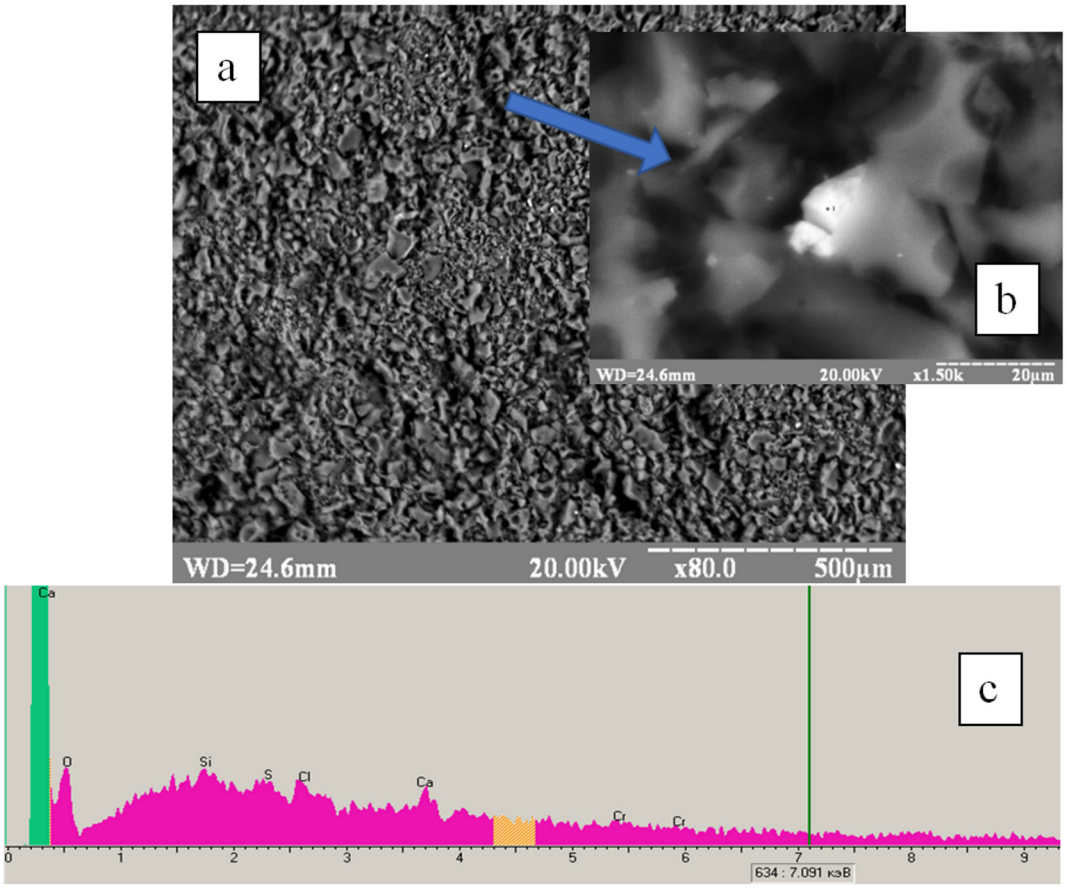

Fig. 3. Surface morphology in secondary electron mode at magnifications of ×80 (a) and ×1500 (b)

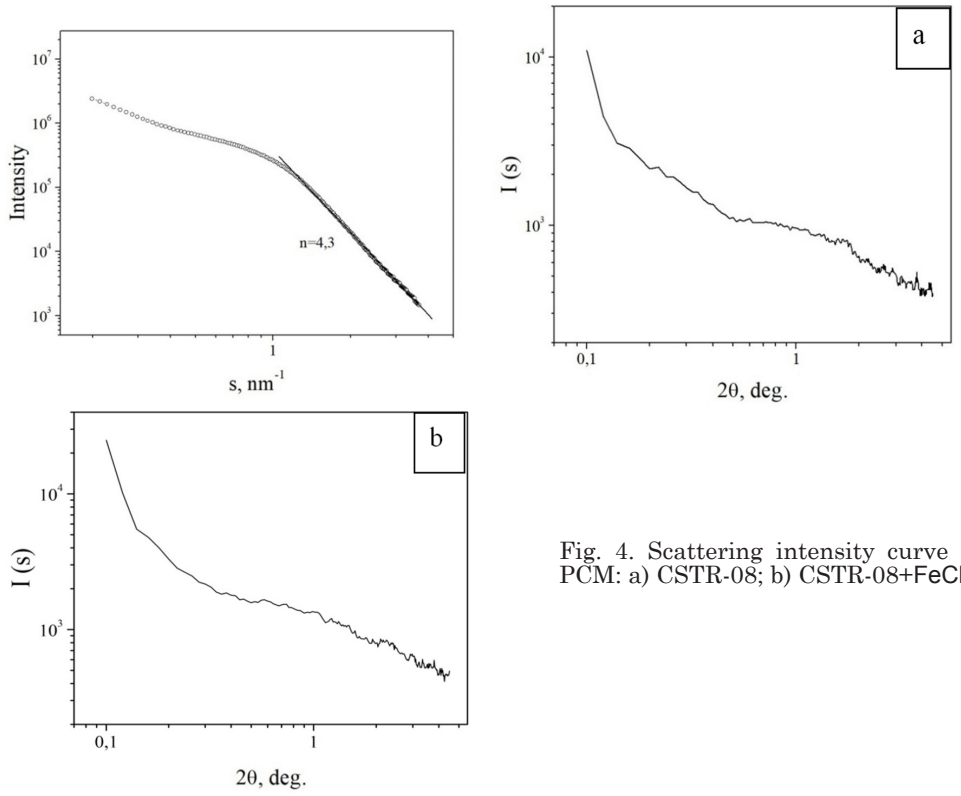

Fig. 4. Scattering intensity curve of PCM: a) CSTR-08; b) CSTR-08+$FeCl_3$

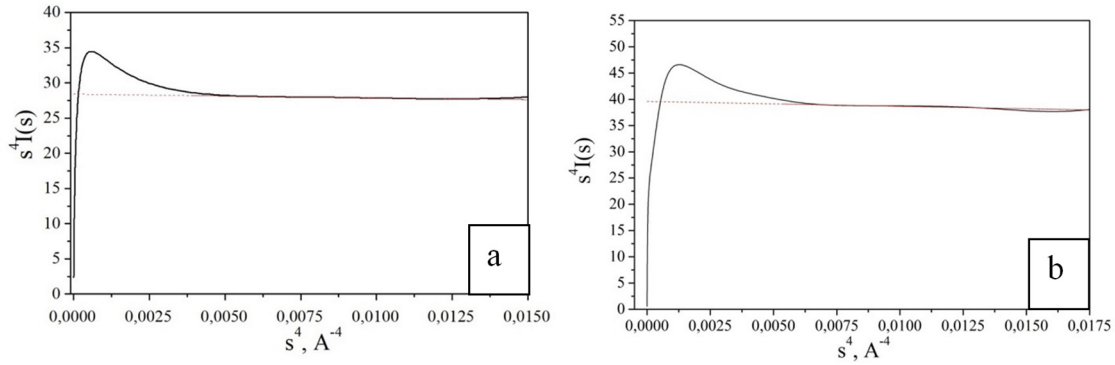

Fig. 5. Scattering intensity curve of chemically pure (a) and $FeCl_3$-modified (b) porous carbon material CSTR-08 plotted in Porod coordinates

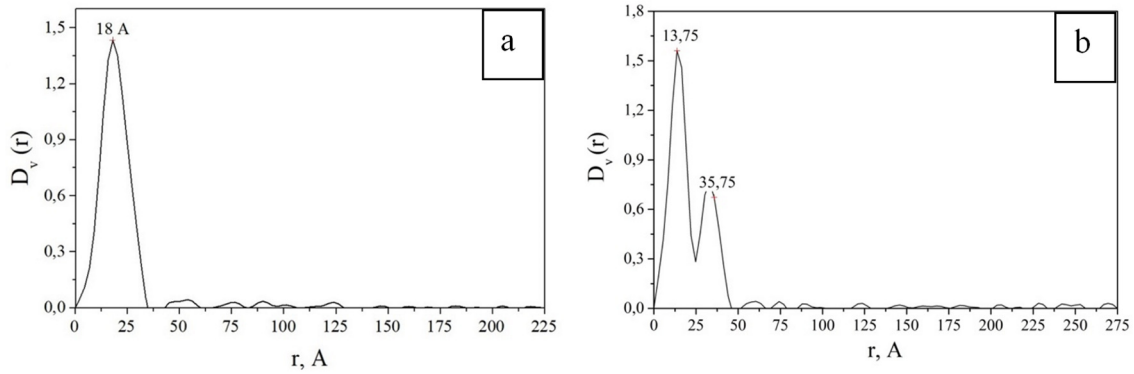

Fig. 6. Pore radius distribution functions of carbon material: a) CSTR-08; b) CSTR-08+$FeCl_3$

of a linear decrease in the scattering intensity curve within the range of wave vector values $s = 1.2 – 3.5$ nm^{-1}, corresponding to the average pore sizes from 0.9 to 2.6 nm. This is confirmed by pore radius distribution functions. The dependence slope indicator $n = 4.3$ falls into the interval of $n = 4$-6, indicating the formation of a diffusive (blurred) surface between the pores and the carbon matrix. This is likely caused by the adsorption of impurity elements at the interface.

Analysis of the intensity curves, plotted in Porod coordinates (Fig. 5) reveals that this carbon feedstock is characterized by a smooth interface between the pores and the carbon matrix. From the scattering intensity graphs, the density of the CSTR-08 carbon material was determined as $\rho_m = 0.12$ g/cm^3, and $\rho_m = 0.43$ g/cm^3 for the $FeCl_3$-modified CSTR-08 material. It can be observed that the modification with iron chloride leads to an increase in the density of the carbon sample CSTR-08 compared to the chemically pure material, due to a higher pore quantity with radii of 25-50 Å and consequently, a larger nano-pore area.

It is evident from the dependence graph of the radius distribution function (Fig. 6a), that pores with a radius of 18 Å predominate in the CSTR-08 sample. There is an increase in the pore radius, and two peaks in the pore distribution curve are observed with radii of 13.7 Å and 35.75 Å for the $FeCl_3$-modified CSTR-08 sample (Fig. 6b). Moreover, the mesopore contribution is almost imperceptible for both samples, as confirmed by results of the complementary DFT method of adsorption porosimetry.

Fig. 7 shows the pore size distribution determined by the DFT method for the CSTR-08 carbon material and the CSTR-08 sample chemically modified with $FeCl_3$. It is interesting to note that the DFT method allows one to calculate the specific surface area, the total pore volume, as well as their size and volumetric distribution. From the obtained data, it is noticeable that the CSTR-08 nanopores and micropores in the size range of 1.1 – 5 nm contribute to the specific surface area and total pore volume.

The SAS results made it possible to calculate the main parameters of the porous structure of the studied materials. For instance, from $s^4 I(s) = f(s^4)$ curves it is possible to calculate the Porod constant K_p [17]. By highlighting the linear sections at $s \to \infty$ on the graphs, you can determine the parameter K_p using the least squares method. Once the Porod constant is determined, the Porod invariant can be calculated using formula (3):

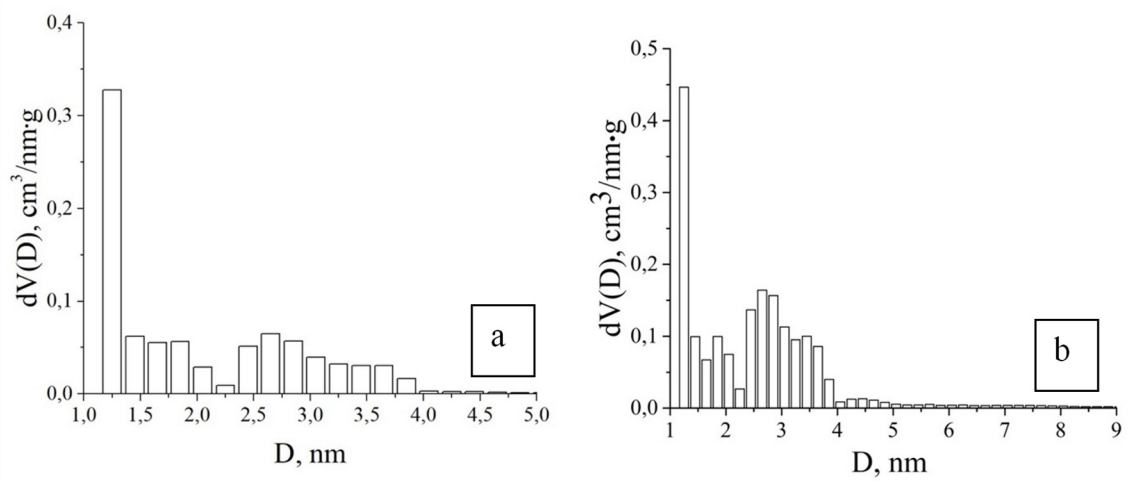

Fig. 7. Pore size distribution of CSTR-08 carbon material: a) before chemical modification b) after chemical modification

$$Q_\rho = \int_0^{s_{\max}} s^2 I(s)\,ds + \frac{K_p}{s_{\max}}, \qquad (3)$$

where s_{max} is the maximum value of the wave vector.

For both the original CSTR-08 and the $FeCl_3$-modified sample, this parameter is in the range of 465 to 470 Å^{-3}. It is worth noting that the value of the integral Porod invariant allows for a qualitative assessment of the total pore volume of the carbon samples. For both samples, the value of K_p is the same and equals 28.0 Å^{-4}, and this is a principal result, since the Porod constant K_p is proportional to the total surface area of the pores according to formula (4):

$$\frac{S}{m} = \pi w(1-w)\frac{K_p}{\rho_m Q_p}, \qquad (4)$$

where w is the volume fraction of pores, and ρ_m is the real density of the material.

The chemical modification of the CSTR-08 with $FeCl_3$ leads to an increase in the specific surface area (S = 1875 m²/g) compared to the original sample (S = 742 m²/g). This is likely associated with the development of narrow pores, an increase in the proportion of pores with diameters of 2.5-4 nm, and the enhancement of porosity. This is evidenced by the increased pore volume fraction for the chemically modified carbon material w = 0.95, compared to the original CSTR-08 carbon material where w = 0.81.

4. Conclusions

The study revealed that the chemical modification of the original carbon material with $FeCl_3$, followed by thermal activation at 700°C in an argon atmosphere, leads to the formation of highly porous carbon material. The results of scanning electron microscopy revealed the presence of carbon grains ranging from 40 to 100 nm with predominantly micro-porous structure. Moreover, an integral analysis of the elemental composition has identified the following chemical elements on the surface of the carbon sample: O in bound form, Si, S, Cl, and Cr.

The analysis of the porous structure of carbon material using complementary methods of adsorption porosimetry and small-angle X-ray scattering has made it possible to establish optimal conditions for synthesizing PCM with well-developed micro-porous structures and the pore size distribution in the range of 1 to 5 nm. The contribution of mesopores to the total pore volume is insignificant for both types of samples. It has been determined that during the $FeCl_3$ modification of the carbon material, the dehydrogenation of fixed carbon structures occurs, leading to the development of internal material porosity. This modification results in an increased volume fraction of pores and an augmented specific surface area for the chemically modified porous carbon material.

Acknowledgments

The work was supported by Project 0121U108649 of the Ministry of Education and Science of Ukraine.

References

1. H. Marsh, F. Rodriguez-Reinoso, Activated Carbon, Elsevier Ltd, Amsterdam (2006).
2. Y. Zhang, G. Qiu, R. Wang et al., *Molecules* **26**, 6014 (2021).
3. L. Wei, G. Yushin, *Nano Energy*, **1**, 552 (2012).
4. J. Rouquerol, F. Rouquerol, P. Llewellyn et al., Adsorption by Powders and Porous Solids: Prin-

ciples, Methodology and Applications, 2nd ed.; Elsevier Inc, Amsterdam (2013).
5. S. Qiu, Z. Chen, H. Zhuo et al., *ACS Sustainable Chemistry & Engineering*, **7**, 15983 (2019).
6. Yu.V. Tamarkina, I.B. Frolova, V.O. Kucherenko. *Water and Water Purification Technologies. Scientific and Technical News,* **29**, 36 (2021).
7. I.M. Budzulyak, V.M.Vashchynskyi, B.I. Rachiy, *Fizychna inzheneriya poverkhni*, **13**, 84 (2015) [in Ukrainian].
8. A.M. Abioye, F.N. Ani, *Renewable and Sustainable Energy Reviews*, **52**, 1282 (2015).
9. V.I. Mandzyuk, I.F. Myronyuk, V.M. Sachko, I.M. Mykytyn, *Surface Engineering and Applied Electrochemistry,* **56**, 93 (2020) [in Russian].
10. J. Bedia, M. Penas-Garzon, A. Gomez-Aviles, J. Rodriguez, C. Belver, *Journal of Carbon Research*, **6**, 21 (2020).
11. J. Bedia, M. Penas-Garzon, A. Gomez-Aviles, J. Rodriguez, C. Belver, *Journal of Carbon Research*, **4**, 63 (2018).
12. N. Ye, Z. Wang, S. Wang, W.J.G.M. Peijnenburg, *Nanotoxicology*, **12**, 423 (2018).
13. A.M. Holmes, L. Mackenzie, M.S. Roberts, *Nanotoxicology,* **14**, 263 (2020).
14. G. Qiu, Y. Guo, J. Xu, et al., *International Journal of Energy Research,* **46**, 22971 (2022).
15. V.M. Vashchynskyi, I.V. Semkiv A.I. Kashuba et al., *Chemistry, Physics & Technology of Surface*, **13**, 349 (2022) [in Ukrainian].
16. S.K.Theydan, M.J. Ahmed, *Powder Technology*, **224**, 101 (2012).
17. V.M. Vashchynskyi, A.M. Boychuk, Ya.B. Vashchynska *Journal of Nano- and Electronic Physics*, **11**, 03012 (2019).